Transportation Research Part C 51 (2015) 196–209

Contents lists available at ScienceDirect

Transportation Research Part C

journal homepage: www.elsevier.com/locate/trc

Operation of signalized diamond interchanges with frontage roads using dynamic reversible lane control

Jing Zhao [a], Yue Liu [b,*], Xiaoguang Yang [c,1]

[a] University of Shanghai for Science and Technology, 516 Jungong Road, Shanghai, PR China
[b] Department of Civil and Environmental Engineering, University of Wisconsin at Milwaukee, P.O. Box 784, Milwaukee, WI, United States
[c] Key Laboratory of Road and Traffic Engineering of the Ministry of Education, 4800 Cao'an Road, Shanghai, PR China

ARTICLE INFO

Article history:
Received 14 May 2013
Received in revised form 23 October 2014
Accepted 30 November 2014
Available online 29 December 2014

Keywords:
Signalized diamond interchange
Capacity
Reversible lane
Binary-Mixed-Integer-Linear-Program

ABSTRACT

Signalized diamond interchanges (SDI), connecting major highways and surface streets in urban and suburban areas, are probably the most widely used interchange patterns. The limited storage space between the two closely joined intersections coupled with heavy traffic volumes may easily oversaturate the facility and cause spillback problems, especially with the presence of frontage roads. This paper presents an innovative design and operational model for SDI by dynamically reversing certain lanes in the internal link on a regular basis with the deployment of overhead reversible lane control signs. A Binary-Mixed-Integer-Linear-Program (BMILP) is formulated to simultaneously optimize lane markings, dynamic usage of the reversible lane, and signal timings for the new SDI system. Results from extensive numerical analyses reveal the promising property of the proposed design and operational model in expanding capacity and reducing congestion at the SDI with frontage roads.

1. Introduction

Diamond interchanges are the probably the most commonly used interchange patterns in urban and suburban areas, connecting major highways and surface streets with two closely spaced intersections. When traffic demand is high, intersections need to be signalized and may become the bottleneck due to the limited spacing between them. Therefore, signalized intersections are often the key operational elements within the interchange system (Fang and Elefteriadou, 2006).

Spacing between intersections at a diamond interchange typically ranges from less than 120 m to 240 m or more (TRB, 2000). Such proximity creates a number of interactive effects that complicate the operation (Xu et al., 2010). It limits the storage capacity available for queued turning vehicles and may induce spillback problems on the internal link. Blockages and delays due to queue spillback can then prevent vehicles at the upstream intersection from reaching the downstream stop line, resulting in inefficient utilization of green times. During traffic demand peak periods, such interactions may finally cause traffic gridlock at adjacent intersections. To address these challenges, it is essential to develop more efficient lane utilization and signal control strategies to operate the two closely space signalized intersections.

In review of literature, this unique operational problem at diamond interchanges was conventionally addressed by optimizing signal control plans (Messer and Chang, 1987; Chaudhary and Chu, 2000; Tian, 2004), falling into two general

* Corresponding author. Tel.: +1 414 229 3857.
E-mail addresses: jing_zhao_traffic@163.com (J. Zhao), yueliu1980@gmail.com (Y. Liu), yangxg@mail.tongji.edu.cn (X. Yang).
[1] Tel./fax: +86 (21) 6958 9475.

http://dx.doi.org/10.1016/j.trc.2014.11.010
0968-090X/

categories: namely the three-phase control (Munjal, 1971; Messer et al., 1977) and the four-phase control (Engelbrecht et al., 2001; Engelbrecht and Barnes, 2003; Gordon and Tighe, 2005; Pham et al., 2011). As shown in Fig. 1, the three-phase control treats the diamond interchange as two separate intersections, each having three phases. One phase is for through movements on the surface street, the second for through and left movements from the internal links and the third for ramp movements. Three-phase operation is efficient if turning traffic volumes are light, and can minimize the cycle length. However, as turning volumes increase, this plan can lead to internal queue spillback and operational breakdown (Gordon and Tighe, 2005). The four-phase control could avoid most queuing problems by giving each of the four approaches from which interchange traffic originates a clear phase through both intersections. However, because it requires four phases, longer cycle lengths are needed which may reduce the capacity of the intersection (Fang, 2004). Moreover, it generally decreases the effective green time per cycle ratio for major movements, resulting higher expected delays than a three-phase control plan (TRB, 2000; Nelson et al., 2000).

When a diamond interchange is oversaturated with high left-turn demand, the conventional treatment of providing left-turn bays with protected left-turn phases may not be sufficient to avoid long delays. Researchers have been looking for unconventional interchange designs to squeeze more capacity out of a diamond interchange with oversaturated traffic conditions. As one of the most popular unconventional interchange designs, Diverging Diamond Interchange (DDI) has received increasing attention in recent years due to its cost-effectiveness over a traditional diamond interchange design. The key logic of DDI is to provide efficient navigation for both left-turn and through movements between highway ramps, and to accommodate left-turning movements onto the arterial without using a left-turn bay (Yang et al., 2013). As shown in Fig. 2, the reverse operations of the through traffic between two ramp terminals in a DDI design allow its left-turn traffic flows from the freeway off-ramps to the opposing flows at each sub-intersection (Edara et al., 2005). With such an assignment of flow movements, a DDI design can significantly reduce the number of traffic conflict points. And there is a great potential of the DDI to yield a better performance over the conventional SDI in increasing capacity and reducing delay primarily due to its efficient two-phase signal operation (Chlewicki, 2003; Bared et al., 2005; Smith and Speth, 2008; Bared, 2009; Maji et al., 2013). However, the DDI concept also has some disadvantages, such as: (a) most of these analyses are based on the assumption that the freeway frontage roads do not exist, or there is no need to facilitate vehicular travel between the freeway off-ramp and on-ramp, for a signalized diamond interchanges with frontage roads (SDI-FR), a third phase should be added to accommodate the through movements on the frontage roads (Martinez and Cheu, 2012), hence the advantages of DDI are undermined; (b) it requires additional construction and permanent changes in layout, which cannot be turned on and off as needed; and (c) the reverse operations of the through traffic in the internal link in a DDI design may cause serious driving errors, especially the wrong-way violations, which may result in an increase in crashes.

One assumption underlying the above operational models is that the geometric layout, including the number of lanes on different directions in the internal link as well as lane markings at intersection approach lanes, is given as an exogenous input and will not change throughout the operation process. However, when an intersection is oversaturated with high traffic demand, the conventional signal control models may not be sufficient to avoid long delays at the signalized diamond interchanges. Furthermore, due to spatial and environmental limitations, it is becoming increasingly difficult to improve diamond interchange operations through geometric improvements.

A further examination of current SDI operation reveals that the large and unbalanced left-turning traffic volume coupled with limited spacing and turning lanes on the internal link contributes most to its failure. Realizing this problem, this research develops a new way to significantly improve the operation of the SDI using dynamic reversible lanes (DRL) in the internal link. The basic concept is to set all the left-turn lanes in the internal link as reversible by using overhead reversible lane control signs. These lanes have the flexibility to be used by different directions during different periods of a signal cycle depending on left-turn volumes and patterns. Such a design would enable a dynamic and integrated utilization of the internal link space and signal green times, resulting a substantial increase of the internal link capacity without the need of major construction.

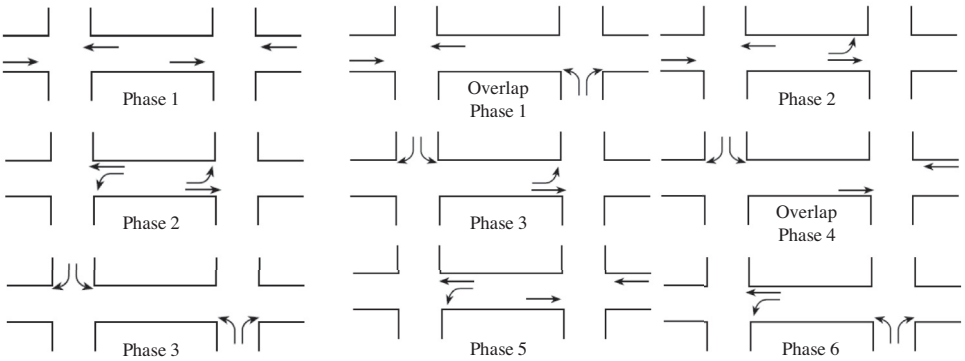

(a) Common three-phase plan (CTP) (b) Texas Transportation Institute four-phase plan (TTI)

Fig. 1. Common signalization schemes for diamond interchanges (TRB, 2000).

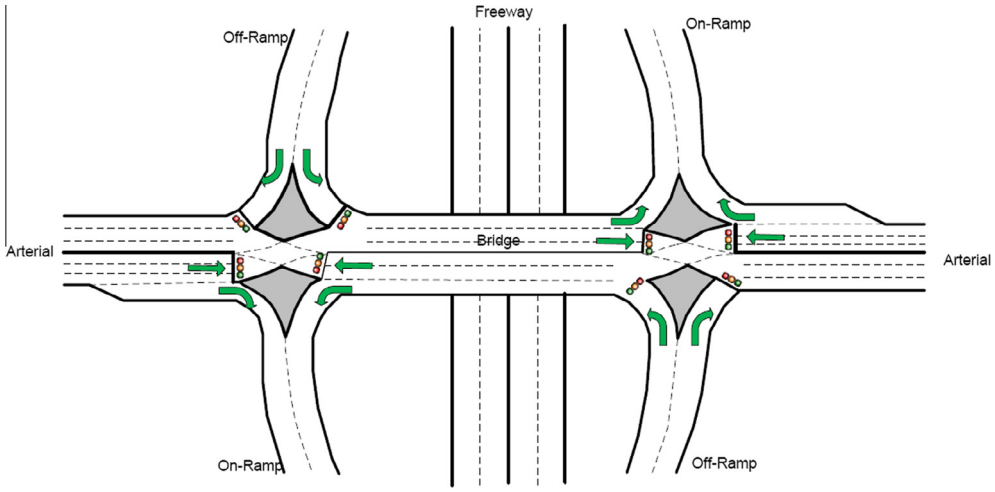

Fig. 2. Geometric layout of DDI design (Yang et al., 2013).

The idea of the reversible lane operation has been well accepted by practitioners in many other applications. The principle is to configure the lanes of a roadway to match available capacity with varying traffic demand. One of the earliest applications of reversible roadways was in Los Angeles in 1928, with a convertible lane variant known as off-center lane movement (Dorsey, 1948). Over the past decades, many different forms of reversible roadways have been used throughout the world to address a variety of needs (Wolshon and Lambert, 2004), including accommodating traffic demand associated with frequent and predictable unbalanced peak-period travel times (Upchurch, 1975; Agent and Clark, 1980; Karoonsoontawong and Lin, 2011; Nava et al., 2012), special event management (Gillis, 1990; Lambert and Wolshon, 2002; Wojtowicz and Wallace, 2010; Hua et al., 2013), and emergency evacuation (Wolshon, 2001; Theodoulou and Wolshon, 2004; Xie and Turnquist, 2011; Ren et al., 2012).

Different from previous studies and applications, this study proposes to operate reversible lanes at the internal link of a signalized diamond interchanges with frontage roads (SDI-FR) on a dynamic and regular basis. A mathematical model is further formulated to simultaneously optimize the lane markings, the dynamic usage of reversible lanes, and the signal timing plans to achieve the best operational performance of the SDI.

The rest of the paper is organized as follows. In Section 2, the basic concept of signalized diamond interchanges with dynamic reversible lanes (DRL) are illustrated. The integrated optimization model based on the DRL concept is formulated in Section 3. Evaluation of the proposed model performance is conducted in Section 4 through extensive numerical and simulation analyses. Conclusions and recommendations are given at the end of the paper.

2. The DRL control concept

The basic concept and operation of dynamic reversible lanes (DRL) at the signalized diamond interchange is illustrated in Fig. 3. All the left-turn lanes in the internal link are set as reversible, and can be used by left-turn traffic from different directions during different periods in a signal cycle. Such design will increase the effective number of lanes used by left-turn traffic thereby allocating more green time for other traffic movements and increasing the overall SDI capacity accordingly.

Fig. 4 further details the operational cycle of the proposed DRL system under the typical TTI four-phase control plan for SDI. The dynamic reversible lanes are reserved as the left-turn lanes for the eastbound direction during the green phase of arm 2 through and arm 5 left turn, while used as the left-turn lanes for westbound direction during the green phase of arm 6 through and arm 1 left turn. An animation of the proposed DRL system operating at a SDI can be found at url: "https://www.dropbox.com/s/tlha4p4dedl19nt/SDI%20WITH%20DRL.mp4". Note that the reversible lanes can only serve one movement direction in a signal phase, so the three-phase control plan is not compatible with the DRL. Furthermore, the overlapping design in the TTI four-phase scheme is good for the queue storage and clearance in the reversible lanes and can further improve the operational efficiency and safety of the proposed DRL system compared with the traditional four-phase scheme without overlaps.

3. The optimization model for DRL operation

To maximize the operational efficiency of the proposed DRL system at the signalized diamond interchange, an optimization model combining the design of the lane markings, dynamic reversible lane usage, and signal timings is developed in this section.

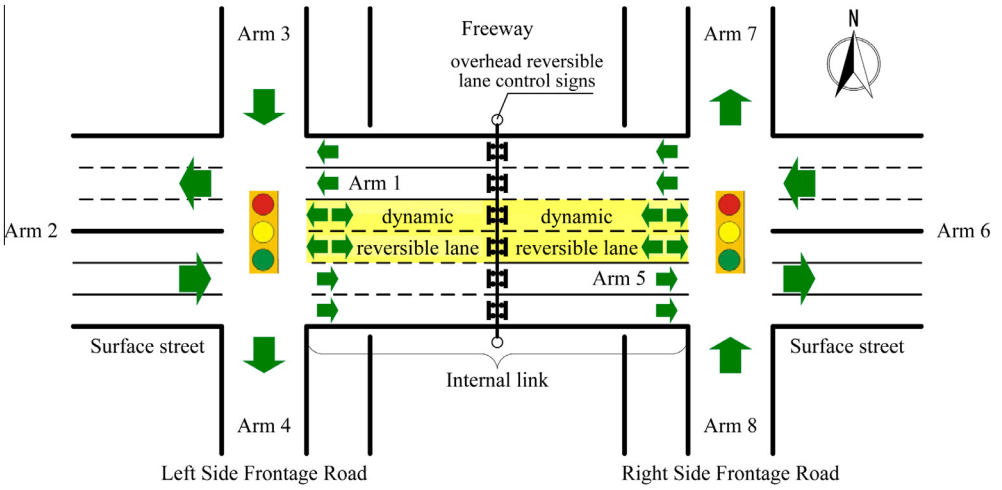

Fig. 3. Signalized diamond interchanges with dynamic reversible lanes (DRL).

3.1. Notations

To facilitate model presentation, notations used hereafter are summarized in Table 1.

3.2. Objective function

The proposed DRL system aims to maximize the reserved capacity at the SDI. By adopting the commonly used assumption that the proportions of the traffic demand remain constant, maximizing the reserve capacity is equivalent to maximizing the common flow multiplier (Gallivan and Heydecker, 1988; Wong and Wong, 2003; Wong and Heydecker, 2011; Zhao et al., 2013), μ, given by:

$$\max \mu \tag{1}$$

3.3. Constraints

The optimization problem shall include the flow conservation constraints,

$$q_{iw} = \sum_{(o,d)} \delta_{iw}^{od} q_{od}, \quad \forall i \in A,\ w \in T_i \tag{2}$$

$$\mu q_{iw} = \sum_{k=1}^{n_{if}+n_{ir}} q_{iwk}, \quad \forall \forall i \in A,\ w \in T_i \tag{3}$$

the right-of-way constraints,

$$M x_{iwk} \geqslant q_{iwk} \geqslant 0, \quad \forall i \in A,\ w \in T_i,\ k \in \{1, \ldots, n_{if} + n_{ir}\} \tag{4}$$

the lane assignment constraints,

$$\sum_{w \in T_i} x_{iwk} \geqslant 1, \quad \forall i \in A,\ k \in \{1, \ldots, n_{if} + n_{ir}\} \tag{5}$$

$$n = n_{1f} + n_{5f} + n_r \tag{6}$$

$$n_{1r} = n_{5r} = n_r \tag{7}$$

$$n_{ir} = 0, \quad \forall i \in A \setminus \{1, 5\} \tag{8}$$

$$x_{i1k} = 1, \quad \forall i \in \{1, 5\},\ k \in \{1, \ldots, n_{ir}\} \tag{9}$$

$$x_{i2k} = 0, \quad \forall i \in \{1, 5\},\ k = \{1, \ldots, n_{ir}\} \tag{10}$$

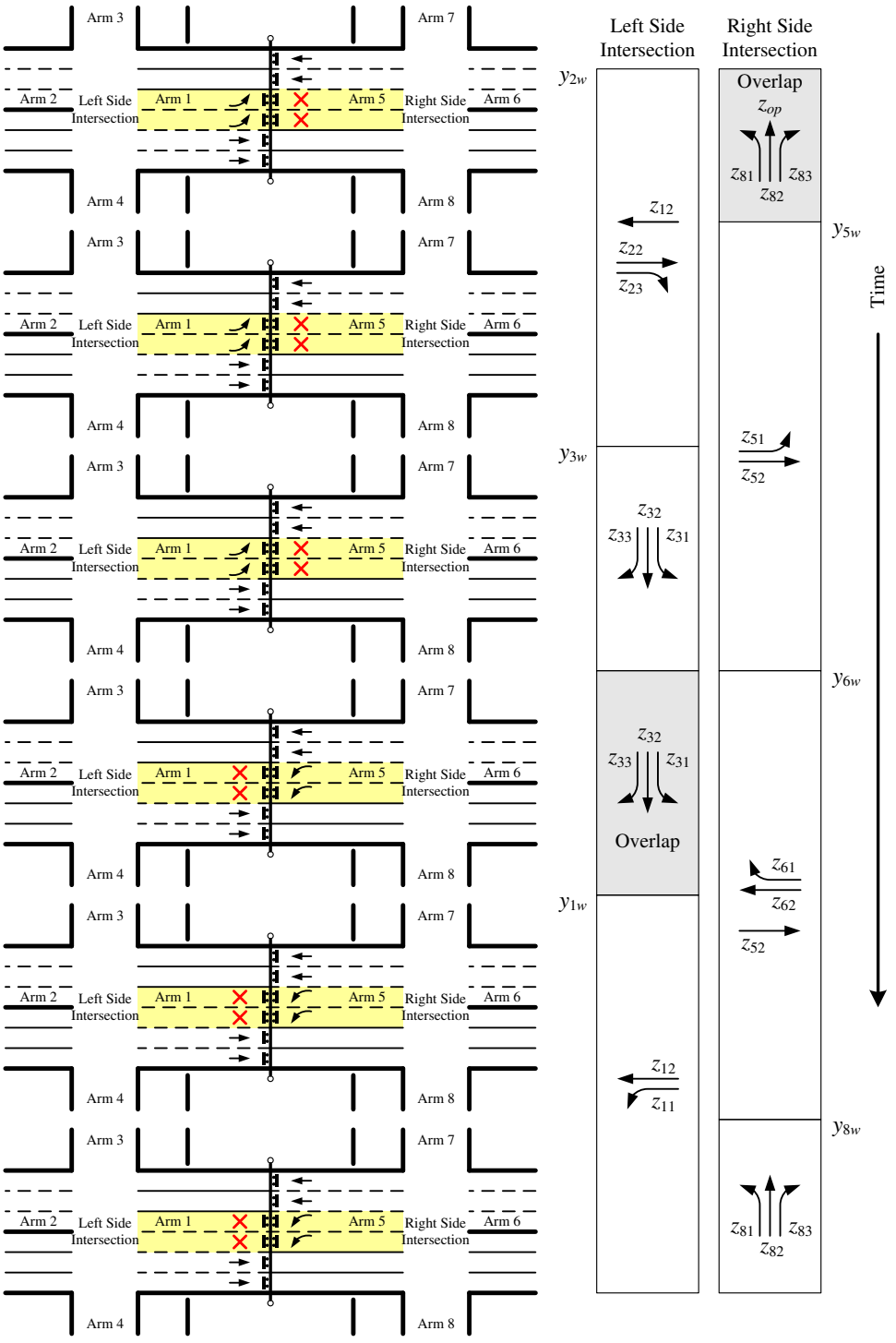

Fig. 4. Operation of dynamic reversible lanes at SDI.

$$x_{i3k} = 0, \quad \forall i \in \{1,5\},\ k = \{1,\ldots,n_{ir}\} \tag{11}$$

$$n^{e}_{iw} \geqslant \sum_{k=1}^{n_{if}+n_{ir}} x_{iwk}, \quad \forall i \in A,\ w \in T_i \tag{12}$$

Table 1
Notation of key model parameters and variables.

Sets and parameters	
A	Set of arms at the SDI
$i, j \in A$	Index of arms
N	Set of demand origins and destinations at the SDI
(o, d)	An OD pair between origin o and destination d, $\forall o, d \in N$
T_i	Set of turning movements on arm i
$w \in T_i$	Index of turning movements on arm i, $w = 1$ for left-turn, $w = 2$ for through movement, and $w = 3$ for right-turn
k	Index of lanes, numbering from the left most lane
δ_{iw}^{od}	A binary indicator showing if the OD pair (o, d) makes turning w on arm i (1 – Yes, 0 – No)
L	Length of the internal link (m)
n	Number of lanes on the internal link
n_{ir}	Number of reversible lanes used as approach lanes on arm i
n_{iw}^{e}	Number of lanes on the exit that receives turning w on arm i
q_{iwk}	Flow of movement w on arm i using lane k (vph)
q_{iw}	Flow of movement w on arm i (vph)
q_{od}	Flow from demand origin o to destination d (vph)
γ_{ik}	Flow ratio of lane k on arm i
s_{ik}	Saturation flow rate of lane k on arm i (vph)
v	Average speed on the internal link (m/s)
$v_{\min}$	Minimum speed on the internal link (m/s)
$\bar{d}$	Average space headway for queuing vehicles on the internal link (m)
$ds_{\max}$	Maximum acceptable degree of the saturation
C	Main-signal cycle length (s)
$C_{\min}, C_{\max}$	Minimum and maximum cycle length (s)
$g_{iw}^{\min}$	Minimum duration of green for movement w on arm i (s)
$I_{iw,jw'}$	Clearance time for a pair of conflicting traffic movements (s), $w \in T_i$, $w' \in T_j$
Decision variables	
n_r	Number of reversible lanes on the internal link
n_{if}	Number of fixed approach lanes on arm i
x_{iwk}	A binary variable indicating the permission of movement w on lane k on arm i
ξ	Reciprocal of main-signal cycle length (1/s)
y_{iw}	Start of green for movement w on arm i
Y_{ik}	Starts of green on lane k on arm i
z_{iw}	Green time ratio for movement w on arm i
Z_{ik}	Green time ratio for lane k on arm i
z_{op}	Green time ratio for the overlap phase at the right-side intersection, as shown in Fig. 2

$$1 - x_{iw(k+1)} \geqslant x_{iw'k}, \quad \forall i \in A,\ w \in \{1,2\},\ w' \in \{w+1,\ldots,3\},\ k \in \{1,\ldots,n_{if}+n_{ir}-1\} \tag{13}$$

the signal timing constraints,

$$\frac{1}{C_{\min}} \geqslant \xi \geqslant \frac{1}{C_{\max}} \tag{14}$$

$$1 \geqslant y_{iw} \geqslant 0, \quad \forall i \in A,\ w \in T_i \tag{15}$$

$$1 \geqslant z_{iw} \geqslant g_{iw}^{min}\xi, \quad \forall i \in A,\ w \in T_i \tag{16}$$

$$M(1 - x_{iwk}) \geqslant Y_{ik} - y_{iw} \geqslant -M(1 - x_{iwk}), \quad \forall i \in A,\ w \in T_i,\ k \in \{1,\ldots,n_{if}+n_{ir}\} \tag{17}$$

$$M(1 - x_{iwk}) \geqslant Z_{ik} - z_{iw} \geqslant -M(1 - x_{iwk}), \quad \forall i \in A, w \in T_i, k \in \{1,\ldots,n_{if}+n_{ir}\} \tag{18}$$

$$y_{2w} = 0, \forall w \in \{2,3\} \tag{19}$$

$$y_{3w} = z_{22} + I_{22,31}, \quad \forall w \in \{1,2,3\} \tag{20}$$

$$y_{1w} = y_{32} + z_{32} + I_{31,11}, \quad \forall w \in \{1,2\} \tag{21}$$

$$y_{11} + z_{11} + I_{11,22} = 1 \tag{22}$$

$$z_{12} = z_{11} + z_{22} + I_{11,22} \tag{23}$$

$$z_{22} = z_{23} \tag{24}$$

$$z_{31} = z_{32} = z_{33} \tag{25}$$

$$y_{5w} = z_{op}, \quad \forall w \in \{1,2\} \tag{26}$$

$$y_{6w} = z_{op} + z_{51} + I_{51,62}, \quad \forall w \in \{2,3\} \tag{27}$$

$$y_{8w} = y_{62} + z_{62} + I_{62,81}, \quad \forall w \in \{1,2,3\} \tag{28}$$

$$y_{81} + z_{81} + I_{81,51} - z_{op} = 1 \tag{29}$$

$$z_{52} = z_{51} + z_{62} + I_{51,62} \tag{30}$$

$$z_{62} = z_{63} \tag{31}$$

$$z_{81} = z_{82} = z_{83} \tag{32}$$

$$y_{11} \geqslant y_{62} + \frac{L}{v}\xi \tag{33}$$

$$y_{51} \geqslant y_{22} + \frac{L}{v}\xi \tag{34}$$

the acceptable level-of-service constraints,

$$M(2 - x_{iwk} - x_{iw(k+1)}) \geqslant \gamma_{i(k+1)} - \gamma_{ik} \geqslant -M(2 - x_{iwk} - x_{iw(k+1)}), \quad \forall i \in A,\ w \in T_i,\ k \in \{1, \ldots, n_{if} + n_{ir}\} \tag{35}$$

$$ds_{\max} Z_{ik} \geqslant \gamma_{ik}, \quad \forall i \in A,\ k \in \{1, \ldots, n_{if} + n_{ir}\} \tag{36}$$

the internal link reversible lane constraints,

$$s_{ik} Z_{ik} \geqslant u \cdot ds_{\max} \cdot q_{iwk}, \quad \forall i \in \{1,5\},\ w \in \{1\} \tag{37}$$

$$y_{11} + z_{11} \geqslant y_{62} + z_{62} + \frac{L}{v_{\min}}\xi \tag{38}$$

$$y_{51} + z_{51} \geqslant y_{22} + z_{22} + \frac{L}{v_{\min}}\xi \tag{39}$$

the internal link overflow avoidance constraints,

$$\frac{L}{\bar{d}} \geqslant \frac{\frac{q_{11}}{\sum_{w=2}^{3} q_{6w}} \sum_{k=1}^{n_{6f}} s_{6k} \left(y_{11} - y_{62} - \frac{L}{v_{min}}\xi\right) s_{1k}}{3600\left(\sum_{k=1}^{n_{1r}} s_{1k} - \frac{q_{11}}{\sum_{w=2}^{3} q_{6w}} \sum_{k=1}^{n_{6f}} s_{6k}\right)}, \quad \forall k \in \{1, \ldots, n_{1r}\} \tag{40}$$

$$\frac{L}{\bar{d}} \geqslant \frac{\frac{q_{62} - q_{11}}{\sum_{w=2}^{3} q_{6w}} \sum_{k=1}^{n_{6f}} s_{6k} \left(y_{11} - y_{62} - \frac{L}{v_{min}}\xi\right) s_{1k}}{3600\left(\sum_{k=n_{1r}+1}^{n_{1f}+n_{1r}} s_{1k} - \frac{q_{62} - q_{11}}{\sum_{w=2}^{3} q_{6w}} \sum_{k=1}^{n_{6f}} s_{6k}\right)}, \quad \forall k \in \{n_{1r} + 1, \ldots, n_{1f} + n_{1r}\} \tag{41}$$

$$\frac{L}{\bar{d}} \geqslant \frac{\frac{q_{51}}{\sum_{w=2}^{3} q_{2w}} \sum_{k=1}^{n_{2f}} s_{2k} \left(z_{op} - \frac{L}{v_{min}}\xi\right) s_{5k}}{3600\left(\sum_{k=1}^{n_{5r}} s_{5k} - \frac{q_{51}}{\sum_{w=2}^{3} q_{2w}} \sum_{k=1}^{n_{2f}} s_{2k}\right)}, \quad \forall k \in \{1, \ldots, n_{5r}\} \tag{42}$$

$$\frac{L}{\bar{d}} \geqslant \frac{\frac{q_{22} - q_{51}}{\sum_{w=2}^{3} q_{2w}} \sum_{k=1}^{n_{2f}} s_{2k} (z_{op} - \frac{L}{v_{min}}\xi) s_{5k}}{3600\left(\sum_{k=n_{5r}+1}^{n_{5f}+n_{5r}} s_{5k} - \frac{q_{22} - q_{51}}{\sum_{w=2}^{3} q_{2w}} \sum_{k=1}^{n_{2f}} s_{2k}\right)}, \quad \forall k \in \{n_{5r} + 1, \ldots, n_{5f} + n_{5r}\} \tag{43}$$

and non-negative constraints for all decision variables listed in Table 1.

Constraint (2) obtains the turning flows given the set of demand origins and destinations as an exogenous input; Constraint (3) indicates that the sum of sub-flows of a movement on different lanes should be equal to the total flow of that

movement. Constraint (4) sets the assigned lane flow q_{iwk} to 0 if the movement w on lane k at arm i is not permitted (i.e.,$x_{iwk} = 0$), where M presents an arbitrary large positive constant number.

Constraint (5) limits the minimum number of permitted movements on traffic lanes, which allows each lane to carry at least one movement; Constraint (6) sets the total number of lanes in the internal link, which is equal to the sum of the number of fixed approach lane on arms 1 and 5, and the number of reversible lanes in the internal link; Constraints (7), (8) gives the number of reversible lanes on each arm. Note that reversible lanes on arms 1 and 5 can be used as left-turn lanes, while other arms have no reversible lanes; Constraints (9)–(11) restrict that only left turns are permitted to use reversible lanes in the internal link, otherwise, it is hard to control the vehicles in the reversible lanes and not good for safety; Constraint (12) sets that the number of lanes at a movement's corresponding exit arm shall be at least as many as the total number of lanes assigned to permit such a movement to prevent the bottleneck and undesirable traffic merging activities; Constraint (13) prevents internal conflicts among lanes at an arm: for any two adjacent traffic lanes, k (left-hand) and $k + 1$ (right-hand) lanes from arm i, if the traffic movement of turn w is permitted on lane $k + 1$, then traffic movements of all other turns, $w + 1, \ldots, 3$, should be prohibited on lane k to eliminate potential internal-cross conflicts within an arm.

Constraint (14) limits the common cycle length for the two sub-intersections at the SDI to be within $C_{\min}$ and $C_{\max}$. According to (Wong and Wong, 2003; Wong and Heydecker, 2011), instead of defining the cycle length directly as the control variable, its reciprocal $\xi = 1/C$, is used to preserve the linearity in the mathematical formulation; Constraint (15) confines the starts of the green to be within a fraction between 0 and 1 of the cycle length; Constraint (16) indicates that the green time ratio of a movement is subject to the minimum duration of green; Constraints (17), (18) defines the lane signal timings. More specifically, if a lane is shared by more than one movement, these movements must receive identical signal indication to avoid ambiguity. According to the TTI's four-phase signalization scheme for diamond interchange, the left intersection at the SDI should be subject to Constraints (19)–(25) for its signal operation; while Constraints (26)–(32) defines the phase structure for the right intersection of the SDI according to TTI's scheme. Constraints (33), (34) determine the length of the overlap phase at both intersections at the SDI.

Constraint (35) sets the flow ratios on a pair of adjacent approach lanes to be identical if they share a common lane marking; γ_{ik} is the flow ratio of lane k on arm i which can be calculated with $\gamma_{ik} = \frac{\sum_{w \in T_i} q_{iwk}}{s_{ik}}, \quad \forall i \in A,\ k \in \{1, \ldots, n_{if} + n_{ir}\}$. Constraint (36) limits the degree of saturation for each approach to be no more than the maximum limit to ensure acceptable level of service.

Since the reversible lanes in the internal link could only serve one direction in a signal phase, for safety clearance purpose, all the left-turn vehicles entering the reversible lanes shall be discharged during the corresponding downstream signal's left-turn phase. Constraint (37) ensures that the corresponding left-turn capacity at the downstream intersection should be greater than the volume entering the reversible lanes u is a safety marginal factor greater than 1.0 to prevent overflow and improve safety and reliability of the reversible lane operations. Constraints (38), (39) are set to ensure safe clearance of vehicles in the reversible lanes in the internal link.

During the DRL operation, overflow in internal link shall be prevented. Therefore, the back-of-queue for movements (1,1), (1,2), (5,1), and (5,2) should always be shorter than the length of the internal link, given by Constraints (40)–(43), respectively. The back-of-queue can be calculated with (TRB, 2000).

3.4. Solution

The above optimization model for DRL operation is a Binary-Mixed-Integer-Linear-Program (BMILP) and can be solved by the standard branch-and-bound routine to global optimal considering the limited number of variables for just two intersections at an SDI.

4. Numerical examples

In this section, the performance of the SDI with DRL control is evaluated through numerical tests. The optimization results obtained from the proposed model will be first compared with conventional plans, including the TTI's four-phase operation (TTI) and the common three-phase operation (CTP) under different traffic demand levels. The impact of various SDI geometric configurations and traffic patterns on the DRL operation is also investigated through sensitivity analysis.

4.1. Performance evaluation

A signalized diamond interchange with three approach lanes and three exit lanes on each arm and six lanes in the internal link is used as an example to evaluate the performance of the proposed DRL control model. Length of the internal link is 100 m. $ds_{\max}$ is set to be 0.9, $C_{\min}$ and $C_{\max}$ are set to be 60 s and 120 s, $\bar{d}$ is set as 7 m, s_{ik} is set to 1800 vphpl for all lanes, u is set to be 1.1, v is set to 12.5 m/s, $v_{\min}$ is set to 10 m/s, and clearance time for any pair of conflicting traffic movements is set to be 4 s. Three traffic demand levels (low, medium, and high) are designed for the test, as summarized in Table 2.

The control plans and performance of the DRL are compared with TTI and CTP under all demand levels. To make a fair comparison between the proposed DRL and other control plans, we have applied the developed model to optimizing lane markings for TTI and CTP, and use TRANSYT-7F to optimize their signal timings. Since there is no existing integrated design

Table 2
Traffic demand levels.

(*o*,*d*)		(2,4)	(2,6)	(2,7)	(3,2)	(3,4)	(3,6)	(6,2)	(6,4)	(6,7)	(8,2)	(8,6)	(8,7)
Volume (vph)	Low	250	400	350	350	300	350	400	350	250	350	350	300
	Medium	375	600	525	525	450	525	600	525	375	525	525	450
	High	450	720	630	630	540	630	720	630	450	630	630	540

for TTI and CTP, the conventional enumeration method is used to produce the optimal design results, whereby an initial layout is determined and then the signal timing is calculated. Although it is not a perfect method, enumeration method is applied to ensure that every possible lane markings for TTI and CTP are tried, and for each lane marking scheme, TRANSYT-7F is used to optimize their signal timings. Therefore, it is ensured that the optimal design results for TTI and CTP could be produced for a fair comparison. In this way, capability flexibility of the DRL can be identified from the comparison. Figs. 5–7 display the optimized lane markings for DRL, TTI, and CTP from the model, and Table 3 shows the optimized signal timings.

The simulation package VISSIM is used as the unbiased evaluator to capture the stochastic variation of traffic flow and evaluate the performance of different control strategies. To overcome the stochastic nature of a microscopic simulation system, an average of 20 simulation runs has been used. Three performance indices, including the total throughput, the average vehicular delay, and the maximum queue length in the internal link, have been selected to compare DRL, TTI and CTP under different demand levels. Simulation and comparison results are shown in Fig. 8.

It can be observed that when traffic demand level is low or medium, all three control plans are comparable in terms of total throughput; while DRL and TTI outperform CTP in average delay and maximum queue lengths. When the demand level is high, the DRL control clearly outperforms TTI and CTP with significantly higher total throughput (11.4% and 13.1% improvement) and lower average delays (68.7% and 70.9% reduction). The maximum queue length in the internal link under the DRL control, though slightly higher compared with the TTI four phase operation, is still within the storage capacity of the internal link. Therefore, by dynamically allocating lanes in the internal link to serve left-turn demands of the two opposite directions, DRL manages to increase the diamond interchange capacity without adding delays greatly. TTI could also avoid

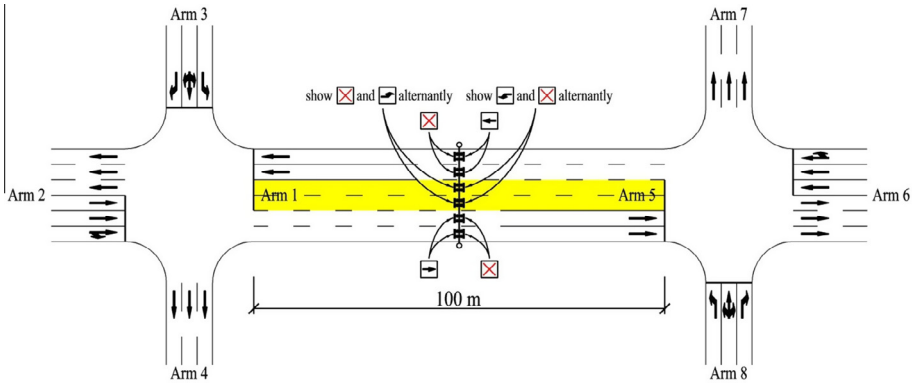

Fig. 5. Optimized lane markings for the DRL control.

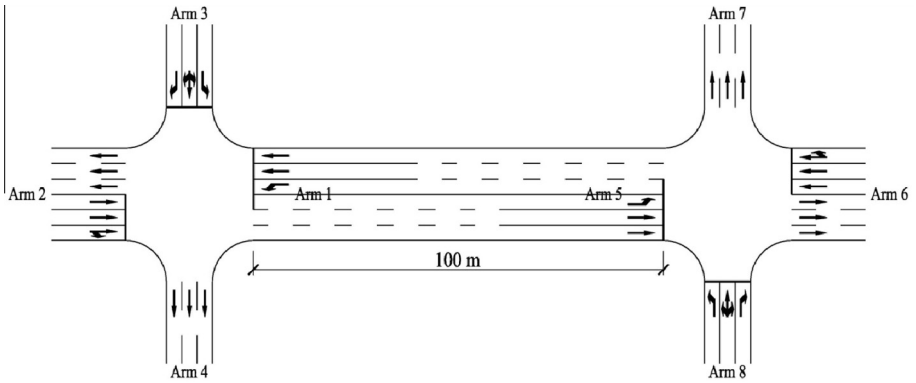

Fig. 6. Optimized lane markings for the TTI control.

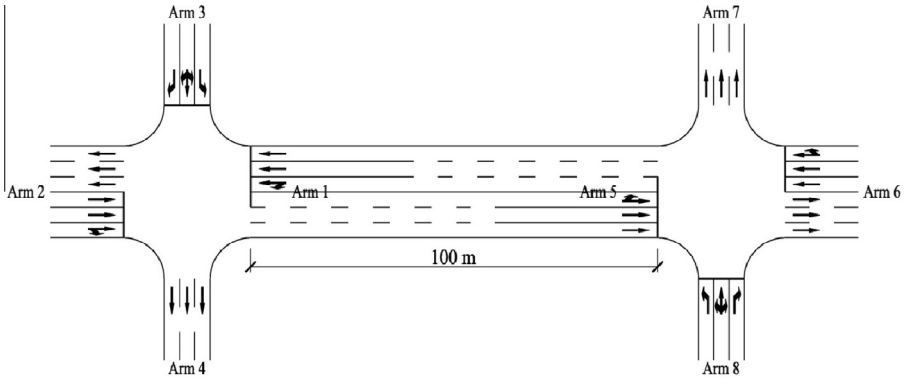

Fig. 7. Optimized lane markings for the CTP control.

Table 3
Optimization results of signal timings.

Arms		1		2		3			5		6		8		
Movements		LT	TH	TH	RT	LT	TH	RT	LT	TH	TH	RT	LT	TH	RT
DRL	Cycle length (s)	120													
	Start of green (s)	92	92	0	0	46	46	46	32	32	60	60	106	106	106
	Duration of green (s)	24	70	42	42	42	42	42	24	70	42	42	42	42	42
	End of green (s)	116	42	42	42	88	88	88	56	102	102	102	28	28	28
TTI	Cycle length (s)	120													
	Start of green (s)	78	78	0	0	39	39	39	18	18	60	60	99	99	99
	Duration of green (s)	38	77	35	35	35	35	35	38	77	35	35	35	35	35
	End of green (s)	116	35	35	35	74	74	74	56	95	95	95	14	14	14
CTP	Cycle length (s)	92													
	Start of green (s)	58	58	0	0	29	29	29	58	58	0	0	29	29	29
	Duration of green (s)	30	30	25	25	25	25	25	30	30	25	25	25	25	25
	End of green (s)	88	88	25	25	54	54	54	88	88	25	25	54	54	54

most queuing problems and yield high intersection throughput by giving each of the four approaches from which interchange traffic originates a clear phase through both intersections, but the delay is significantly higher than the DRL. It should be noticed that the maximum queue length in the internal link of DRL control is relatively high due to the higher frequency of lane allocation, though it can be managed well by the optimization model to ensure reliability of operation.

4.2. Sensitivity analyses

This section investigates the impact of various SDI geometric configurations and traffic patterns on the DRL operation. Table 4 shows the layouts of nine experimental cases. In the sensitivity analysis, we use equal traffic demand at each approach for all cases. Turning fractions at the frontage roads are set to be 35% of left turn, 30% of through, and 35% of right turn. Turning proportion of left turn and through on the surface street is set to range from 5% to 75%, and right turn proportion is set at 25%. All other model parameters are kept the same as in Section 4.1. Performances of DRL, TTI, and CTP are compared under all experimental cases.

Fig. 9 summarizes the analysis results with the *x*-axis of each sub-picture representing the proportion of left-turn (LT) on the surface streets, and the *y*-axis being the resulting reserve capacity of SDI.

One can observe that both DRL and TTI outperform CTP in terms of improving the SDI capacity under all test cases; however their performances are shown to be affected by many factors, including the number of lanes in the internal link, the length of the internal link, and the proportion of left turns. There exhibits an obvious descending trend in SDI capacity under TTI control with the increase of left-turn proportion on the surface-street; while the capacity under DRL remains relatively stable. This is primarily due to the fact that setting dynamic reversible lanes improves the level of flexibility of the SDI to accommodate turning traffic demand. Therefore, the DRL control is shown to outperform the TTI in improving SDI capacity when the left-turn proportion on the surface-street is high.

When the length of the internal link is short (see Fig. 9a–c), the DRL outperforms TTI in terms of SDI capacity. With the increase of the internal link length, the SDI capacity under DRL decreases but the capacity under TTI remains unchanged, indicating that when the internal link is sufficiently long (more than 150 m), the TTI operation is better. This is due to the fact that longer internal link requires increased clearance time for reversible lane operations.

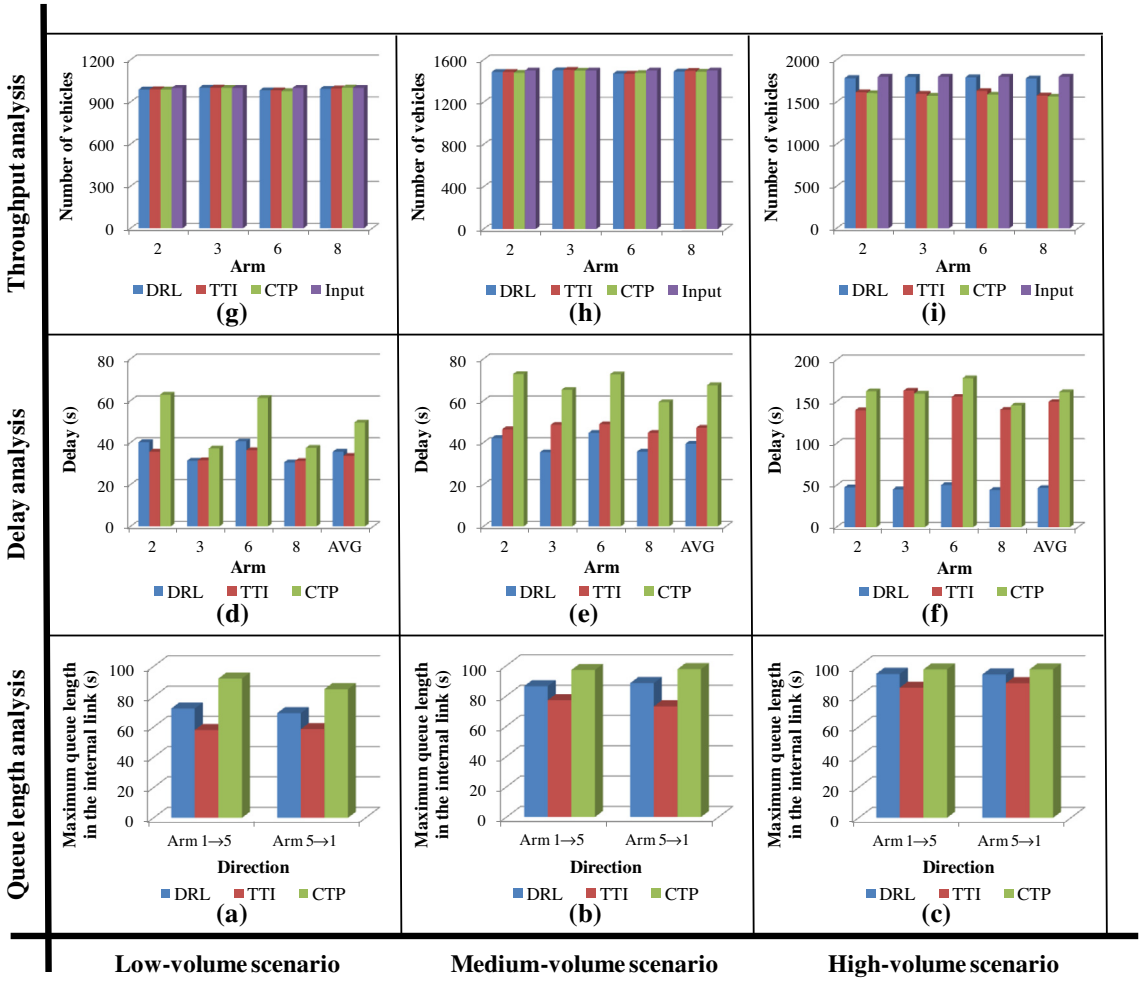

Fig. 8. Performance evaluation results.

Table 4
Experimental cases.

Scenario	Number of approach lanes	Number of exit lanes	Number of lanes in the internal link	Length of the internal link (m)
1	3	3	6	100
2	3	3	7	100
3	4	4	8	100
4	3	3	6	150
5	3	3	7	150
6	4	4	8	150
7	3	3	6	200
8	3	3	7	200
9	4	4	8	200

It is also interesting to find that the DRL has the potential to improve the capacity of SDI even when the number of lanes in the internal link is unequal for both directions. Table 5 summarizes the comparison of throughput at the SDI (the one used in Section 4.1) under the operation of CTP, TTI, and DRL with different number of internal link lanes. The SDI is assumed to be operated under a high traffic demand level shown in Table 6, and is due for an enhancement to improve its current operation. A total of 8 candidate enhancement plans are designed. Plans 1–3 keep the number of lanes in the internal link unchanged and use CTP, TTI, and DRL to operate the SDI; plans 4–6 add only one lane in the internal link and use CTP, TTI, and DRL to operate the SDI; and plans 7–8 add two lanes in the internal link using CTP and TTI. One can observe in Table 5 that the DRL with only one lane added (plan 6) outperforms all other candidate plans in terms of total throughput at the SDI. Even

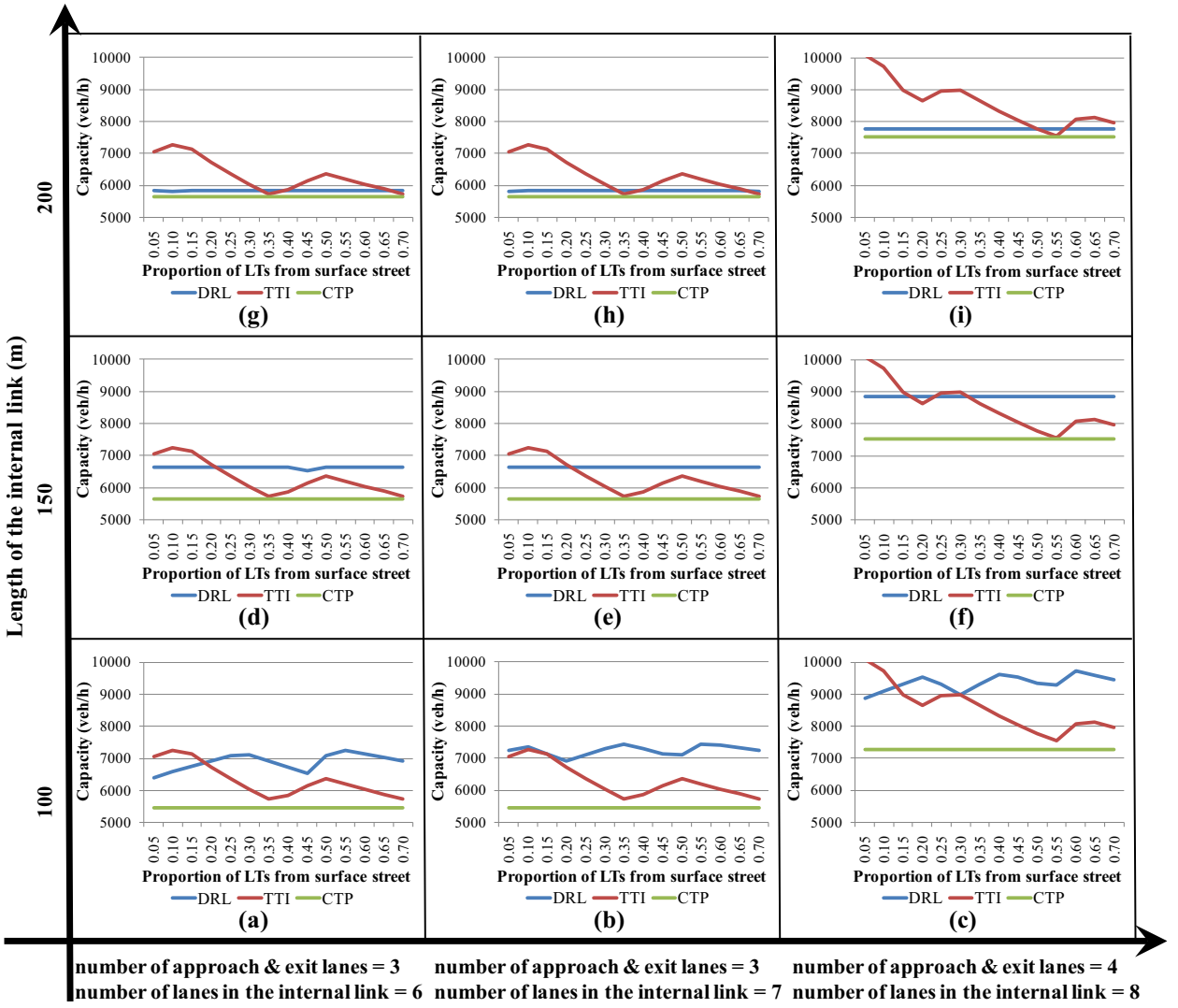

Fig. 9. Performance comparison among DRL, TTI and CTP.

Table 5
Comparison of throughputs at the SDI with different number of internal link lanes.

Plans		Throughput (vehs)	Difference with plan 6 (%)
Plan 1	Original design + CTP (6 lanes in the internal link)	6330	−22.0
Plan 2	Original design + TTI (6 lanes in the internal link)	6421	−20.8
Plan 3	Original design + DRL (6 lanes in the internal link)	7376	−9.1
Plan 4	Adding one lane + CTP (7 lanes in the internal link)	6417	−20.9
Plan 5	Adding one lane + TTI (7 lanes in the internal link)	6504	−19.8
Plan 6	Adding one lane + DRL (7 lanes in the internal link)	8110	0
Plan 7	Adding two lanes + CTP (8 lanes in the internal link)	6761	−16.6
Plan 8	Adding two lanes + TTI (8 lanes in the internal link)	7520	−7.3

Table 6
Traffic demand for throughput analysis.

(o,d)	(2,4)	(2,6)	(2,7)	(3,2)	(3,4)	(3,6)	(6,2)	(6,4)	(6,7)	(8,2)	(8,6)	(8,7)
Volume (vph)	550	880	770	770	660	770	880	770	550	770	770	660

compared with plans that add two lanes in the internal link (plans 7 and 8), plan 6 yields significantly higher throughputs. This is primarily due to the fact that the added one lane could be set as the reversible lane used by different directions during different periods of a signal cycle under the DRL while TTI and CTP only favor the direction with more lanes. Such an advantage of DRL is particularly useful for interchange enhancement where the limited available space prevents the addition of more than one lane in the internal link.

5. Conclusion

A new design and operation of signalized diamond interchange with frontage roads using dynamic reversible lanes is developed in this paper with the objective to increase capacity and relieve congestion at the SDI with limited storage space between the two closely joined intersections coupled with heavy traffic volumes. A Binary-Mixed-Integer-Linear-Program (BMILP) is formulated to simultaneously optimize lane markings, dynamic usage of the reversible lane, and signal timings for the new SDI system. Numerical analyses are conducted to evaluate the performance the proposed design and compared it with the Texas Transportation Institute four-phase plan (TTI) and the common three-phase plan (CTP) under different traffic demand levels and geometric configurations, from which the following conclusions could be drawn:

(1) The new design outperforms CTP under all test scenarios in terms of increasing the capacity of a diamond interchange (up to 37% improvement of capacity). When compared with the TTI control, the new design yields better performance (up to 30% improvement of capacity) when the left-turn proportion on the surface-street exceeds 20% and the length of the internal link is within 150 m. Thus, it is particularly promising for use at diamond interchanges with very limited space for expansion.
(2) The new design is shown to be effective in reducing average delays at the diamond interchange under medium and high traffic demand levels. The highest reduction is achieved at the highest demand level, resulting in 68.7% and 70.9% reduction of delay time compared with TTI and CTP, respectively. Thus, the new design is very promising for use at diamond interchanges experiencing heavy traffic volumes and high delays.
(3) Under high traffic demand levels, substantial improvement in the SDI throughput could be achieved by adding just one lane in the internal link and operating with the DRL. Such an advantage of the new design is particularly useful for interchange enhancement where the limited available space prevents the addition of more than one lane in the internal link.

It should be noted that the new DRL system has the flexibility of working part time in real world applications, only activated when needed (e.g. high volume and overflow). With the advance of vehicle-infrastructure-integration technology, more precise control of vehicles entering the internal link would become possible to further enhance the operational reliability of the new DRL system. However, since the proposed DRL design is new, the ill-intentioned drivers might cause safety problem, careful driver behavior studies and adequate driver education have to be carried out before the new DRL system is perfected and implemented in the field. Vehicle detectors could be used to control vehicles entering the reversible lanes in practice and ensure the operation reliability of the DRL control.

Acknowledgement

The research is supported by the National Natural Science Foundation of China under Grant Nos. 51238008 and 51178345.

References

Agent, K.R., Clark, J.D., 1980. Evaluation of Reversible Lanes (Nicholasville Road; Lexington Kentucky). Technical Report, Kentucky Department of Transportation.
Bared, J.G., Edara, P.K., Jagannathan, R., 2005. Design and operational performance of double crossover interchange and diverging diamond interchange. Transp. Res. Rec. 1912, 31–38.
Bared, J., 2009. Double Crossover Diamond Interchange. FHWA-HRT-09-054. Federal Highway Administration.
Chaudhary, N.A., Chu, C.L., 2000. Guidelines for Timing and Coordinating Diamond Interchanges with Adjacent Traffic Signals. TX-00/4913-2, Texas Transportation Institute.
Chlewicki, G., 2003. New interchange and intersection designs: the synchronized split – phasing intersection and the diverging diamond interchange. In: 2nd Urban Street Symposium, Anaheim, California.
Dorsey, R.T., 1948. The use of the off-center lane movement in Los Angeles. Traffic Quart. 2 (3), 291–302.
Edara, P.K., Bared, J.G., Jagannathan, R., 2005. Diverging diamond interchange and double crossover intersection – vehicle and pedestrian performance. In: 3rd International Symposium on Highway Geometric Design, Chicago Illinois.
Engelbrecht, R.J., Barnes, K.E., 2003. Advanced traffic signal control for diamond interchanges. In: 82nd Annual Meeting of the Transportation Research Board, Washington, DC.
Engelbrecht, R.J., Venglar, S.P., Tian Z.Z., 2001. Research Report on Improving Diamond Interchange Operations using Available Traffic Controller Features. FHWA/TX-02/4158-1, Texas Transportation Institute.
Fang, F., Elefteriadou, L., 2006. Development of an optimization methodology for adaptive traffic signal control at diamond interchanges. J. Transport. Eng. 132 (8), 629–637.
Fang, F., 2004. Optimal Adaptive Signal Control for Diamond Interchanges using Dynamic Programming. Ph.D. Thesis, The Pennsylvania State University, Pennsylvania.

Gallivan, S., Heydecker, B.G., 1988. Optimising the control performance of traffic signals at a single junction. Transport. Res. Part B: Methodological 22 (5), 357–370.
Gillis, R.D., 1990. Unlocking arena gridlock. Civ. Eng. 60 (2), 43–45.
Gordon, R.L., Tighe, W., 2005. Traffic Control Systems Handbook. FHWA-HOP-06-006. Federal Highway Administration.
Hua, J.Y., Ren, G., Cheng, Y., Huang, Z.F., Ran, B., 2013. Corridor management of large planned special events: integrated optimization of park-and-ride and bus contraflow measures. In: 92nd Annual Meeting of the Transportation Research Board, Washington, DC.
Karoonsoontawong, A., Lin, D.Y., 2011. Time-varying lane-based capacity reversibility for traffic management. Computer-Aided Civil Infrastruct. Eng. 26 (8), 632–646.
Lambert, L., Wolshon, B., 2002. Analysis of Reverse Flow Traffic Operations Phase I: Urban Sporting Event Measurement and Evaluation. Technical Report, Louisiana State University.
Maji, A., Mishra, S., Jha, M.K., 2013. Critical lane volume (CLV)-based capacity and level of service analyses for diverging diamond interchange. In: 92nd Annual Meeting of the Transportation Research Board, Washington, DC.
Martinez, J.A., Cheu, R.L., 2012. Double crossover versus conventional diamond interchanges both with frontage roads. J. Transport. Inst. Transport. Eng. 4 (1), 1–17.
Messer, C.J., Chang, M.S., 1987. Traffic operations of basic actuated traffic control systems at diamond interchanges. Transp. Res. Rec. 1114, 54–62.
Messer, C.J., Fambro, D.B., Richards, S.H., 1977. Optimization of pretimed signalized diamond interchanges. Transp. Res. Rec. 644, 78–84.
Munjal, P.K., 1971. An analysis of diamond interchange signalization. Highway Res. Rec. 349, 47–64.
Nava, E., Shelton, J., Chiu, Y.C., 2012. Analyzing impacts of dynamic reversible lane systems using a multi-resolution modeling approach. In: 91st Annual Meeting of the Transportation Research Board, Washington, DC.
Nelson, E.J., Bullock, D., Urbanik, T., 2000. Implementing actuated control of diamond interchanges. J. Transport. Eng. 126 (5), 390–395.
Pham, V.C., Alam, F., Potgieter, J., Fang, F.C., Xu, W.L., 2011. Integrated fuzzy signal and ramp-metering at a diamond interchange. J. Adv. Transport.. http://dx.doi.org/10.1002/atr.167.
Ren, G., Hua, J., Cheng, Y., Zhang, Y., Ran, B., 2012. Bus contraflow lane: improved contraflow approach in freeway evacuation. Transp. Res. Rec. 2312, 150–158.
Smith, S., Speth, S.B., 2008. A comparative analysis of diverging diamond interchange operations. In: ITE 2008 Annual Meeting and Exhibit, Anaheim, California.
Theodoulou, G., Wolshon, B., 2004. Alternative methods to increase the effectiveness of freeway contraflow evacuation. Transp. Res. Rec. 1865, 48–56.
Tian, Z., 2004. Development and Evaluation of Operational Strategies for Providing an Integrated Diamond Interchange Ramp-Metering Control System. Ph.D. Thesis, Department of Civil and Environmental Engineering, Texas A&M University.
Transportation Research Board, 2000. Highway Capacity Manual 2000. Transportation Research Board, Washington, DC.
Upchurch, J., 1975. Reversible flow on a six lane urban arterial. Traffic Eng. 45 (12), 11–14.
Wojtowicz, J., Wallace, W.A., 2010. Traffic management for planned special events using traffic microsimulation modeling and tabletop exercises. J. Transport. Safety Security 2 (2), 102–121.
Wolshon, B., Lambert, L., 2004. Convertible Roadways and Lanes: a Synthesis of Highway Practice. NCHRP Synthesis 340, Transportation Research Board.
Wolshon, B., 2001. "One-way-out": contraflow freeway operation for hurricane evacuation. Natural Hazards Rev. 2 (3), 105–112.
Wong, C.K., Heydecker, B.G., 2011. Optimal allocation of turns to lanes at an isolated signal-controlled junction. Transport. Res. Part B: Methodological 45 (4), 667–681.
Wong, C.K., Wong, S.C., 2003. Lane-based optimization of signal timings for isolated junctions. Transport. Res. Part B: Methodological 37 (1), 63–84.
Xie, C., Turnquist, M.A., 2011. Lane-based evacuation network optimization: an integrated lagrangian relaxation and tabu search approach. Transport. Res. Part C: Emerg. Technol. 19 (1), 40–63.
Xu, H., Liu, H., Tian, Z., 2010. Control delay at signalized diamond interchanges considering internal queue spillback. Transp. Res. Rec. 2173, 123–132.
Yang, X., Chang, G.L., Rahwanji, S., 2013. A multi-stage system for planning analysis and signal design of diverging diamond interchange. In: 92nd Annual Meeting of the Transportation Research Board, Washington, DC.
Zhao, J., Ma, W., Michael Zhang, H., Yang, X., 2013. Increasing the capacity of signalized intersections by dynamically using exit-lanes for left-turn traffic. In: 92nd Annual Meeting of the Transportation Research Board, Washington, DC.